


Effects of environment correlations on the onset of collective decay in waveguide QEDA. Del Ángel ¹, P. Solano,^{2,3} and P. Barberis-Blostein¹¹*Instituto de Investigaciones en Matemáticas Aplicadas y en Sistemas,**Universidad Nacional Autónoma de México, Ciudad Universitaria, 04510, DF, Mexico*²*Departamento de Física, Facultad de Ciencias Físicas y Matemáticas, Universidad de Concepción, Concepción, Chile*³*CIFAR Azrieli Global Scholars Program, CIFAR, Toronto, Canada*

(Received 20 December 2022; accepted 22 May 2023; published 7 July 2023)

We analyze the dynamics of one and two two-level atoms interacting with the electromagnetic field in the vicinity of an optical nanofiber without making either the Born or the Markov approximations. We model the dielectric response of the nanofiber with a constant dielectric function and the Drude-Lorentz model, observing deviations from the standard super- and subradiant decays. We discuss the validity of approximating the speed of atom-atom communication to the group velocity of the guided field in the presence of nontrivial environment correlations. Our work presents a deeper understanding of the validity of commonly used approximations in recent waveguide QED platforms.

DOI: [10.1103/PhysRevA.108.013703](https://doi.org/10.1103/PhysRevA.108.013703)**I. INTRODUCTION**

The theory of open quantum systems studies the interaction of a quantum system with its environment. Through a series of approximations, one can describe the problem with simple equations, which allow for analytical solutions in some particular cases [1–6]. The most common approximations assume that the quantum system never entangles with its environment, known as the Born approximation, and that the evolution timescale of the system is much larger than the evolution of its environment, known as the Markov approximation. Although these approximations accurately describe common scenarios, such as atoms interacting through the electromagnetic environment in free space [7,8], one should question their validity when describing novel experimental configurations beyond what they originally intended to represent. In particular, the rapidly growing field of waveguide quantum electrodynamics (wQED), which describes atoms along a waveguide collectively interacting through the guided field [9–17], is built upon knowledge from open quantum systems. However, the validity of the approximations borrowed from open quantum systems interacting with the free space as their environment should be questioned considering novel experimental configurations [10,11,15] and theoretical proposals [18–24], where the atoms interact with each other at large distances.

Quantitative analyses of atoms interacting with waveguides are intrinsically system-dependent. Without losing sight of the phenomenology, we focus our attention on optical nanofibers (ONFs) [25], a platform that facilitates the interaction of emitters separated by macroscopic distances. Reference [26] derives the Markovian master equation for atoms interacting with an electromagnetic environment in the presence of a nanofiber. The authors assume that the distance between the atoms is negligible and that the environment is Dirac delta correlated. Nevertheless, approximating the correlation functions of the electromagnetic environment with a Dirac delta function is unrealistic since the field emitted by an atom into

the guided modes can strongly affect another at a later time. A correlation function with two Dirac delta functions separated by the delayed interaction time can simplify the problem, interestingly leading to non-Markovian dynamics [18]. Approximating the correlation functions of the electromagnetic environment of a nanofiber with Dirac delta functions is so far a standard procedure in wQED; thus, proving its validity is crucial. Besides estimating quantitative deviations from the predictions, a detailed study of the correlation functions allows for answering fundamental questions. For example, what is the field velocity that accurately describes the delayed interaction time between two atoms: phase or group velocity? What is the timescale and dynamics for the appearance of collective dynamics? Is it possible to observe these effects with current experimental technology?

In this paper we study how the dynamics of two separated two-level atoms is affected by the correlations of the fundamental guided modes of an ONF at zero temperature, which acts as the environment for the atoms. To do so, we calculate and analyze in detail the correlation functions of the guided modes as a function of the separation between atoms. We consider two dispersion relations, a commonly assumed constant dielectric function and the more realistic Drude-Lorentz (DL) model for the nanofiber dielectric function. By numerically solving the dynamical equations, we estimate the modification of the collective decay rates of the atoms and explore the effects of explicitly considering the correlations of the environment.

We show that for a single atom in the vicinity of an ONF at zero temperature, it is unnecessary to modify the spectral density of the environment to render its correlation close to a Dirac delta distribution, contrary to the free space case [1,27]. In such a scenario, the Markovian approximation is valid for the two dielectric functions we consider, a result which, to our knowledge, has not been previously verified despite its widespread use in this context. For two atoms, we observe that the correlation functions for a constant dielectric function

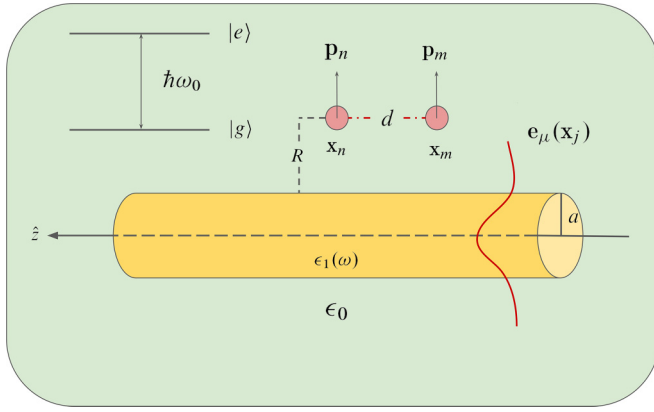


FIG. 1. Schematic representation of the system. Two two-level atoms with resonant frequency ω_0 separated a distance d interact via a common bath, given by the evanescent field of the guided modes \mathbf{e}_μ of an optical nanofiber. The optical nanofiber of radius a is characterized by a dielectric function $\epsilon(\omega)$.

resemble displaced Dirac delta distributions. However, the delayed maxima of the environment correlations are not centered at nor determined by the time it takes the electromagnetic field to propagate between the atoms at the group or phase velocities. Nevertheless, when we study the dynamics of the collective behavior, we obtain that the onset of the collective behavior is consistent with assuming that the atoms interact with a delay given by the group velocity only if the atoms are distant enough. Additionally, we find that atoms prepared in (anti)symmetric states radiate at rates slightly below (above) those obtained with the Markovian approximation, suggesting the impossibility of realizing perfect subradiant states. Our study provides a test for the validity of usual approximations employed in wQED.

Our paper is organized as follows: in Sec. II we present the model for the system and describe how the correlation functions and the atoms' evolution are numerically calculated. In Sec. III we show and discuss the main results of this work, as well as its implications. Finally, we summarize and give an outline in Sec. IV.

II. PHYSICAL MODEL

We consider two identical two-level atoms with resonance frequency ω_0 ($E_e - E_g = \hbar\omega_0$) in the vicinity of an optical nanofiber of radius a and a frequency-dependent dielectric function $\epsilon(\omega)$ (see Fig. 1). We consider two dielectric functions for our study: a commonly assumed constant function $\epsilon_C(\omega) \approx \epsilon_C(\omega_0)$, yielding a constant refractive index $n_1 = \sqrt{\epsilon_C(\omega)/\epsilon_0} \approx 1.4534$, which is a typical value for ONF operating at optical frequencies [25], and the more realistic Drude-Lorentz (DL) dielectric function $\epsilon_L(\omega)/\epsilon_0 = 1 + \omega_p^2[(\omega_R^2 - \omega^2) - i\gamma\omega]^{-1}$, where ω_R and γ are the resonant frequency and decay rate of the constituents of the ONF, respectively, and ω_p is its plasma frequency [28]. We choose a constant dielectric function to emulate the effect of the Markovian approximation in the study of the subsystem and reservoir dynamics. Namely, it singles out the parameters of the reservoir associated with the resonant frequency of the

subsystem as the only relevant one in the overall dynamics. But, of course, it does not describe a realistic media since it would violate Kramers-Kronig relations. In contrast, the DL function is an excellent model to approximate the behavior of many realistic dielectric functions since it exhibits the effects of regular and anomalous dispersion and absorption. The parameters of the DL function are chosen so that they mimic the essential features of silica glass, such as a high absorption for frequencies in the ultraviolet regime and refractive indices close to 1.5 in the optical regime [25]. We take the values of these parameters to be $\omega_R = \omega_{350} = 2\pi c/350 \text{ nm}$ and $\gamma_{350} = 4\alpha a_0^2 \omega_{350}^3 / 3c^2$, corresponding to half of the ultraviolet interval and the decay rate of a single constituent via an electric dipole transition, respectively; the value of the plasma frequency is fixed by setting the refractive index of the ONF to be n_1 at the resonance frequency of the atoms. We neglect the effects of absorption associated with the imaginary part of this function near the atomic resonance.

We study the case in which the atoms couple exclusively with the fundamental mode HE_{11} of the guided field of the ONF by means of electric dipole interactions. In the interaction picture, the atom-field interaction Hamiltonian after the rotating wave approximation (RWA) is given by

$$H_{\text{int}} = i\hbar \sum_{\mu} \sum_{m=1}^2 G_{\mu m} e^{-i(\omega - \omega_0)t} \sigma_m^\dagger a_{\mu} + \text{H.c.}, \quad (1)$$

$$G_{\mu m} = \sqrt{\frac{\omega \beta'}{4\pi \epsilon_0 \hbar}} \bar{p}_m \bar{e}_\mu(\bar{x}_m) e^{i[l_f \beta(\omega) z_m + l \phi_m]}. \quad (2)$$

Here the index $m = 1, 2$ labels an atom in position $\bar{x}_m = (r_m, \phi_m, z_m)$ in cylindrical coordinates, and the sum $\sum_{\mu} = \sum_{l,f} \int_0^\infty d\omega$ goes over the field polarization in the circular basis, the propagation direction along the fiber's axis, and the frequency of the guided modes, which are encoded through the variable $\mu = (l = \pm 1, f = \pm 1, \omega)$; $\sigma_m = |g_m\rangle\langle e_m|$ is the atomic lowering operator, and a_{μ} is the annihilation operator of a photon with parameters μ . The coupling frequencies $G_{\mu m}$ are written in terms of the propagation constant $\beta(\omega)$, the density of states $\beta' = \partial\beta/\partial\omega$, the electric dipole matrix element of the m th atom \bar{p}_m , and the components of the guided field modes \bar{e}_μ , which are explicitly given in Ref. [26]. For each frequency component of the field, the propagation constant of the fundamental mode is obtained by numerically solving the following eigenvalue equations [29]:

$$\frac{J_0(ha)}{haJ_1(ha)} = \left[\frac{n_1^2 + n_2^2}{4n_1^2} \right] \frac{K_1(qa)}{qaK_1(qa)} + \left(\frac{1}{ha} \right)^2 + R(\omega, \beta), \quad (3)$$

$$R(\omega, \beta) = \left\{ \left[\frac{n_1^2 - n_2^2}{4n_1^2} \frac{K_1(qa)}{qaK_1(qa)} \right]^2 + \left[\frac{\beta}{k_1} \left(\frac{1}{(ha)^2} + \frac{1}{(qa)^2} \right) \right]^2 \right\}^{\frac{1}{2}}, \quad (4)$$

where n_j represents the refractive indices of the ONF ($j = 1$) and the vacuum ($j = 2$), $h = \sqrt{k_1^2 - \beta^2}$, $q = \sqrt{\beta^2 - k_2^2}$, $k_j = n_j(\omega)\omega/c$, and J_j, K_j are the j th-order Bessel functions of the first kind and the modified of the second kind, respectively.

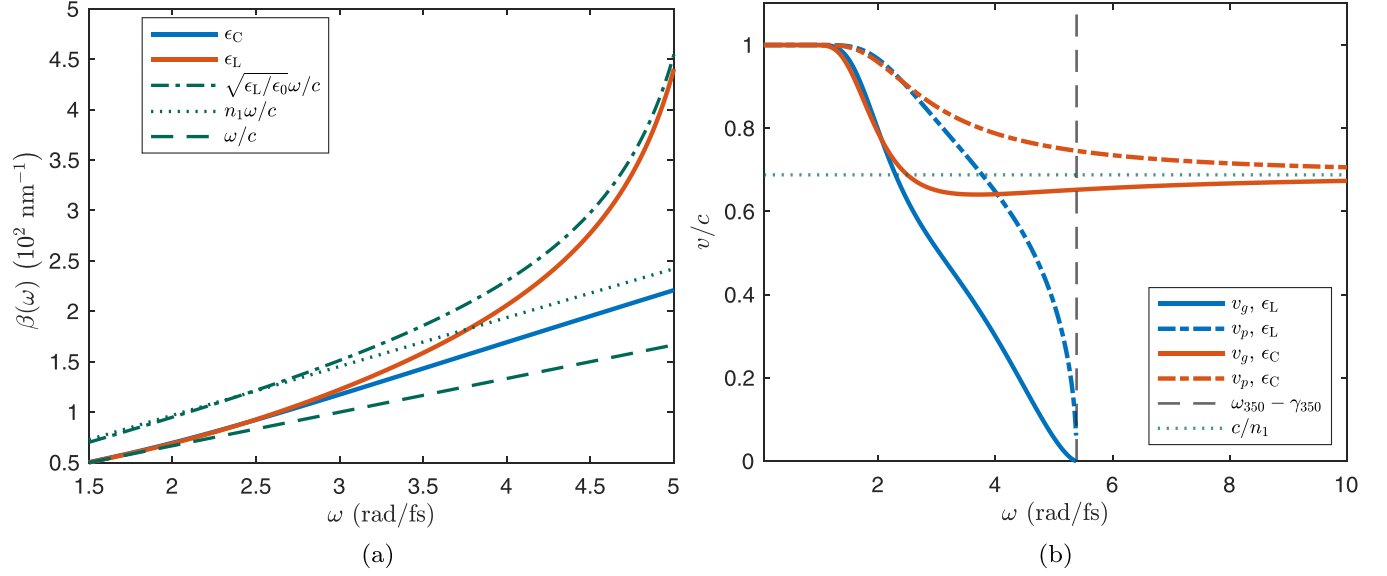


FIG. 2. Dispersion relation (a) and group and phase velocities (b) of the ONF's fundamental mode as a function of the field's frequency and using the constant ϵ_C and Drude-Lorentz ϵ_L dielectric functions. In (a) the solid curves depict the mode's dispersion relation for both dielectric functions, while the dashed lines represent their low- and high-frequency asymptotic behavior corresponding to that of vacuum and an infinite dielectric medium with dispersion relation $n_1(\omega)\omega/c$. In (b) the solid and dashed lines portray the mode's group and phase velocities normalized with respect to c , while the dashed vertical and horizontal lines correspond to the ONF's resonant frequency and the value of the asymptotic velocity when employing the constant dielectric function $v_\infty = c/n_1$, respectively. The set of solid and dashed curves obtained with the constant dielectric function approach c/n_1 as $\omega \rightarrow \infty$, while those calculated with the DL function go to 0 as $\omega \rightarrow \omega_{350} - \gamma_{350}$.

Since the Hamiltonian under the RWA preserves the total excitation number, we consider the evolution of the following state in the single excitation manifold:

$$|\psi(t)\rangle = \sum_{m=1}^2 c_m(t) \sigma_m^\dagger |gg\rangle \otimes |0\rangle + \sum_{\mu} c_{\mu}(t) |gg\rangle \otimes |1_{\mu}\rangle, \quad (5)$$

where c_m and c_{μ} are the atomic and field excitation probability amplitudes, respectively. Assuming that both atoms are prepared with their electric dipoles pointing along the radial direction $\vec{p}_m = \vec{p}_n = p\hat{r}$ and located at the same distance from the surface of the fiber $r_m = r_n = R$, we derive the equation of motion for the atomic amplitudes using Eq. (1). Formally integrating out the field excitation probability amplitudes and substituting them in the equation for c_m we obtain

$$\dot{c}_m(t) = - \sum_{n=1}^2 \int_0^t dt' F_{mn}(t-t') c_n(t'), \quad (6)$$

$$\begin{aligned} F_{mn}(t) &= \sum_{\mu} G_{\mu m} G_{\mu n}^* e^{-i(\omega-\omega_0)t} \\ &= \int_0^{\infty} d\omega e^{-i(\omega-\omega_0)t} S(\omega, R) \\ &\quad \times \cos[\beta(\omega)d] \cos(\phi_m - \phi_n), \end{aligned} \quad (7)$$

$$S(\omega, R) = \left(\frac{|p|^2}{\pi \epsilon_0 \hbar} \right) \omega \frac{\partial \beta}{\partial \omega} |e_r(\omega, R)|^2. \quad (8)$$

Here $S(\omega, R)$ is the one-point spectral density of the guided mode. $F_{mn}(t)$ represents the zero-temperature correlation

function at the position of each atom ($m = n$) and between the two atomic positions ($m \neq n$) separated a distance $d = |z_m - z_n|$ along the ONF and a distance R from its surface. The correlation function is given by the Fourier transform of $S(\omega, R) \cos[\beta(\omega)d] \cos(\phi_m - \phi_n)$. When $m = n$, its real part is associated with the spontaneous decay of a single atom into the fundamental mode and its imaginary part with the Lamb shift induced by the ONF. When $m \neq n$, the correlation function corresponds with the influence one atom exerts on the other, with its imaginary part giving rise to the so-called dipole-dipole interaction. Since the angular coordinates of the atoms are not coupled to the frequency components of the field, the shape of the two-point correlation function is not affected by the particular choice of these coordinates (only its strength), and, therefore, we set $\cos(\phi_m - \phi_n) = 1$. When $F_{mm}(t)$ is a Dirac delta centered at zero and $F_{mn}(t)$ is given by two Dirac deltas displaced by the retarded time, we recover the equations of motion in [18].

III. RESULTS

A. Dispersion relations, spectral density, and correlation functions

In order to calculate the correlation functions $F_{mn}(t)$, we first need to solve Eq. (3) to obtain the dispersion relation $\beta(\omega)$, shown in Fig. 2(a). Since the fraction of the guided electromagnetic field contained inside the dielectric nanofiber is inversely proportional to its wavelength, the dispersion relation of the guided mode is asymptotically bounded between the vacuum one at low frequencies and that of a pure dielectric medium, $n_1(\omega)\omega/c$, at large frequencies. Figure 2(b) shows

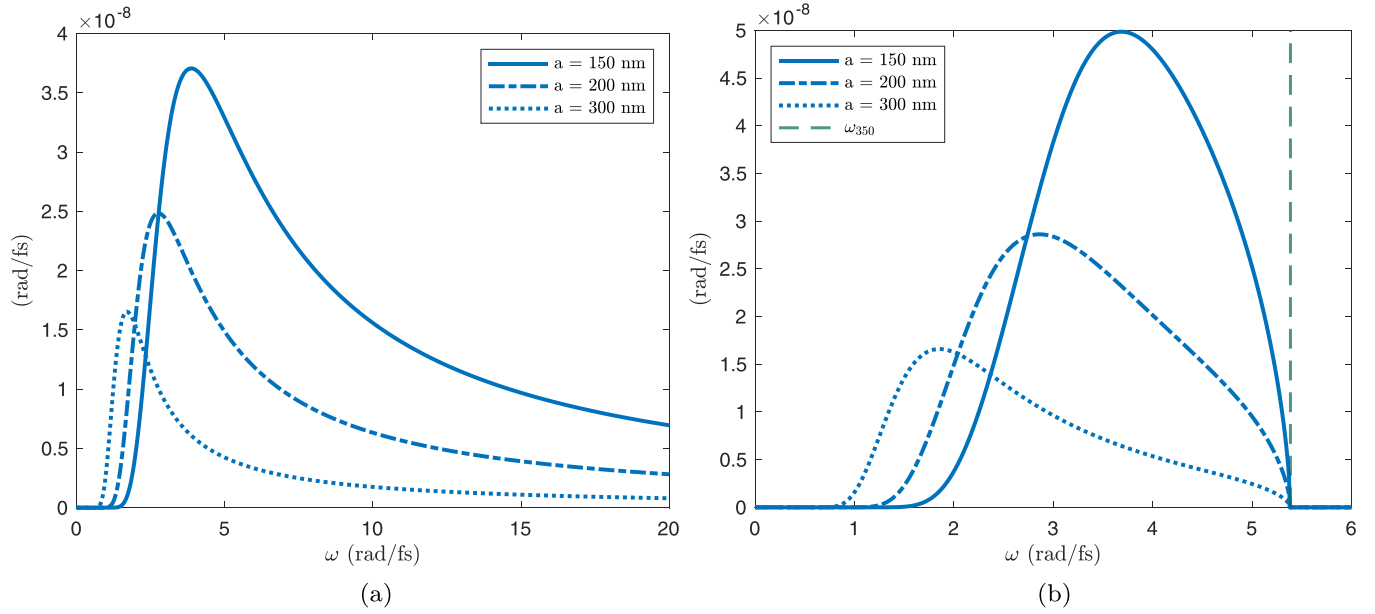


FIG. 3. One-point spectral density $S(\omega, R = 100 \text{ nm})$ for the constant ϵ_C (a) and the DL ϵ_L (b) dielectric functions as a function of the ONF's radius a .

the group $v_g = (\partial\beta/\partial\omega)^{-1}$ and phase $v_p = \omega/\beta$ velocities for both dielectric functions we consider. When using the DL model, both group and phase velocities becomes negligible as the frequency approaches the resonance frequency of the ONF. For frequencies greater than ω_{350} , the anomalous dispersion phenomenon breaks down the guiding condition of the ONF, $n_1(\omega) - n_2 > 0$. On the other hand, when considering a constant dielectric function, the propagation constant $\beta(\omega)$ increases linearly with frequency, and both group and phase velocity coincide, asymptotically approaching the speed of light inside the dielectric, c/n_1 .

Using the numerically calculated $\beta(\omega)$ and Eq. (8) we plot the one-point spectral density $S(\omega, R)$ in Fig. 3. For $T = 0$ the spectral density is the inverse Fourier transform of the correlation function [4], which implies that for the constant dielectric function [see Fig. 3(a)] large frequency contributions lead to correlation functions localized in time. Furthermore, the time-domain correlations in the DL model are much broader since the spectral density cuts off at the resonant frequency of the ONF [see Fig. 3(b)].

We discretize the integration over ω in Eq. (7), allowing us to compute $F_{mn}(t)$ with a fast Fourier transform in an equally spaced time grid $\{t_j | t_j = t_1 + (j-1)\Delta t, j \in \mathbb{N}\}$. The fact that the propagation constant $\beta(\omega)$ becomes large near the dielectric resonance in the DL model complicates the calculation of the two-atom correlation function. The $\cos[d\beta(\omega)]$ factor in the two-point spectral density in Eq. (7) oscillates increasingly fast as the integration approaches the resonant frequency, making its sampling above the Nyquist frequency computationally expensive. In order to resolve this, preventing the phenomenon of aliasing and considering that our field theory is incapable of describing the effects of high absorption and dispersion, we introduce a hard cutoff far below ω_{350} at one of the zeros of the $\cos[d\beta(\omega)]$ factor, which is chosen such that the variation in the results obtained with higher

frequency zeros is negligible [4]. We note that, in contrast to the free space case [30,31], the spectral densities obtained from the guided modes of the ONF do not diverge at high frequencies, producing correlation functions with a finite width even at zero temperature.

Figure 4 shows the real and imaginary parts of the correlation function of the fundamental mode for one and two atoms 100 nm away from the fiber surface separated at the resonant atomic wavelength $d = 780 \text{ nm}$ for a fiber radius of 200 nm. When using a constant dielectric function we obtain single-atom correlation functions with a sharp and well-localized peak at the origin and a two-atom correlation function with two peaks separated by a time difference $t = 2dn_1/c$.

For a constant dispersion relation, the width of the correlation function, which is a measure of the correlation time of the field and one of the sources of non-Markovian effects in the atomic dynamics, is less than 0.05 fs. This implies that, in the case of a single atom, the Markov approximation is justified at zero temperature, a result whose foundation in its vacuum counterpart has been widely discussed by many authors such as Carmichael [30] and demonstrated only recently by Rivas *et al.* [27]. For two atoms, the correlation function has two narrow peaks resembling two Dirac deltas. However, the time interval between them, given by $t = 2dn_1/c$, differs from the intuitive assumption of atom-atom communication at a group velocity, leading to $t = 2d/v_g$. We further investigate this in the next section.

When using the DL dispersion relation the resulting correlations present an oscillatory behavior resembling $\text{sinc}(t)$ functions whose width is approximately 1.5 fs in both the single- and two-atom cases. This validates the Markovian approximation for a single atom. Contrary to the case with a constant dielectric function, it's not clear how to associate a communication time between the atoms. In light of these

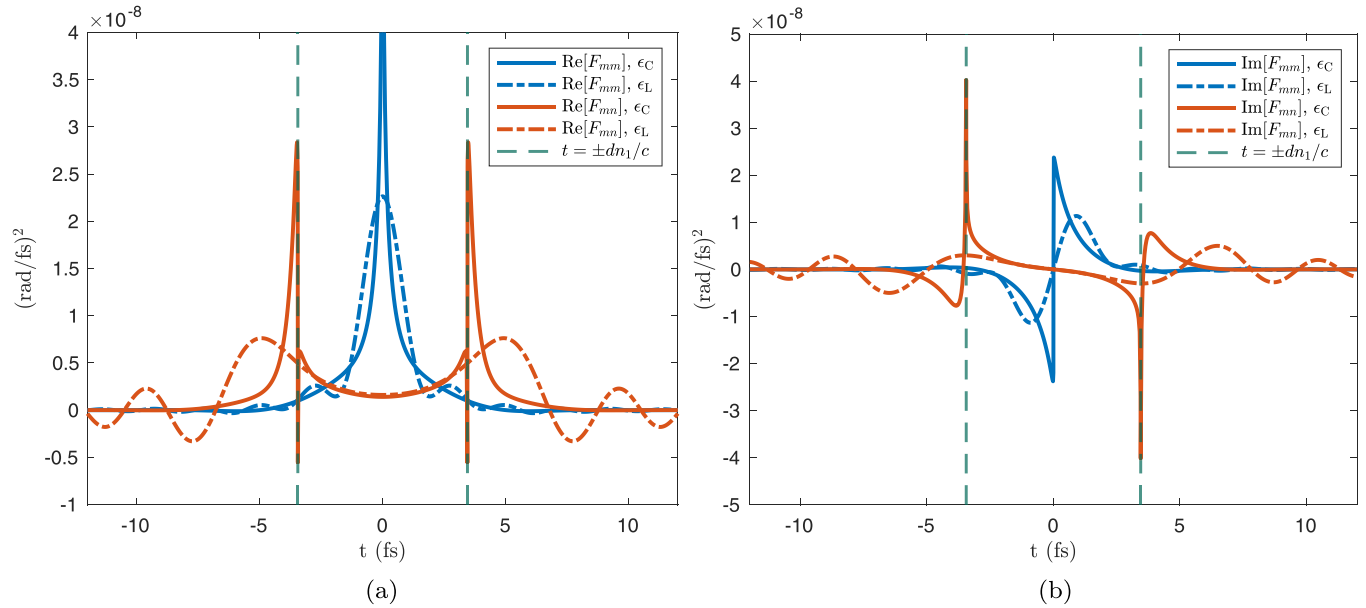


FIG. 4. Real (a) and imaginary (b) parts of the fundamental mode's correlation functions $F_{mn}(t)$ for a 200 nm radius ONF in the presence of one ($m = n$) and two ($m \neq n$) atoms, both separated 100 nm away from the fiber's surface and a distance between them of an atomic resonant wavelength $d = 2\pi/\beta_0 = 780$ nm along the fiber's axis. Here the solid curves depict the correlation functions computed using the constant dielectric function ϵ_C , while the dashed ones portray those obtained with the DL function ϵ_L . Note that for a constant dielectric function the correlation functions have peaks with small widths, resembling Dirac delta functions. For the DL dielectric function the two-atom correlation function has decaying oscillations, and so it is not clear how to approximate with Dirac delta functions.

results, we integrate Eq. (6) to elucidate the influence of the correlation functions on the collective atomic evolution.

B. Atomic dynamics

We solve for the dynamics of two atoms in initially symmetric or antisymmetric states $|\psi_{\pm}\rangle = (|eg\rangle \pm |ge\rangle)/\sqrt{2}$ using the real and imaginary parts of the numerically calculated field correlation functions, which account for the decay rate into the guided mode of the ONF and the atomic energy shifts. We apply the trapezoidal rule twice on the right-hand side of Eq. (6) to numerically solve for the evolution of the atomic excitation probability amplitudes (see the Appendix for details). We analyze our results neglecting the atomic decay into other modes, which is well justified since there is negligible coupling to thermal photons in the limit of zero temperature and optical frequencies, and given the fact that the radiated modes of the waveguide serve as an additional dissipative channel and, therefore, do not contribute to the coherent dynamics of the atoms, which is the focus of our paper.

As Fig. 5 shows, the collective excitation probabilities $|c_{\pm}(t)|^2$ behave as that of independent emitters before the communication between the atoms is established. After that, collective features manifest as decay rates close to twice and zero times the natural decay rate for the symmetric and antisymmetric states, respectively, i.e., super and subradiance. The superradiant decays in Fig. 5(a) display only quantitative differences between both models, while the onset of subradiance inherits the behavior of the correlation functions used to calculate them, as Fig. 5(b) shows. In contrast with the Markovian case, where the collective behavior starts instantaneously

upon atom-atom communication, there is a smooth transition from independent to collective decay. Figure 5(c) shows an example comparing the two behaviors. Note that, although the atoms are prepared in the antisymmetric state, and at distances which are integer multiples of π/β_0 , our solutions predict that they must radiate, even if it is at a rate several orders of magnitude below that of a single atom. This contrasts with the picture established in [18], where the emission process is completely inhibited in this situation.

We estimate the modified collective decay rates from the solutions by fitting the data to a straight line $P(t) = \gamma_{\text{col}}t + P_0$ at times greater than 300 fs so that we can ensure that the collective behavior has been fully established. We show in Fig. 6 the quotient between the symmetric and antisymmetric collective decay rates and that of a single atom as a function of the ONF's radius $\gamma_{\text{col}}/\gamma$. We find that the quotients are independent from the separation between the atoms and that the deviations from what is obtained with the Markovian approximation become apparent for radii approximately less than four times the resonant wavelength of the atomic transition, with variations up to 0.5% and 4% for the DL and constant dielectric functions, respectively. In spite of the minor differences between our results and the predictions given by the Markovian approximation, similar differences of a few percent of the decay rate have been measured for single atoms around an ONF [32]. However, collective effects require a precise positioning of the atoms, hindering its observation for atoms along a nanofiber, but feasible in other wQED platforms. For ONF radii smaller than 150 nm, the calculations were not carried out because of the increasing difficulty involved in computing the dispersion relation of the field.

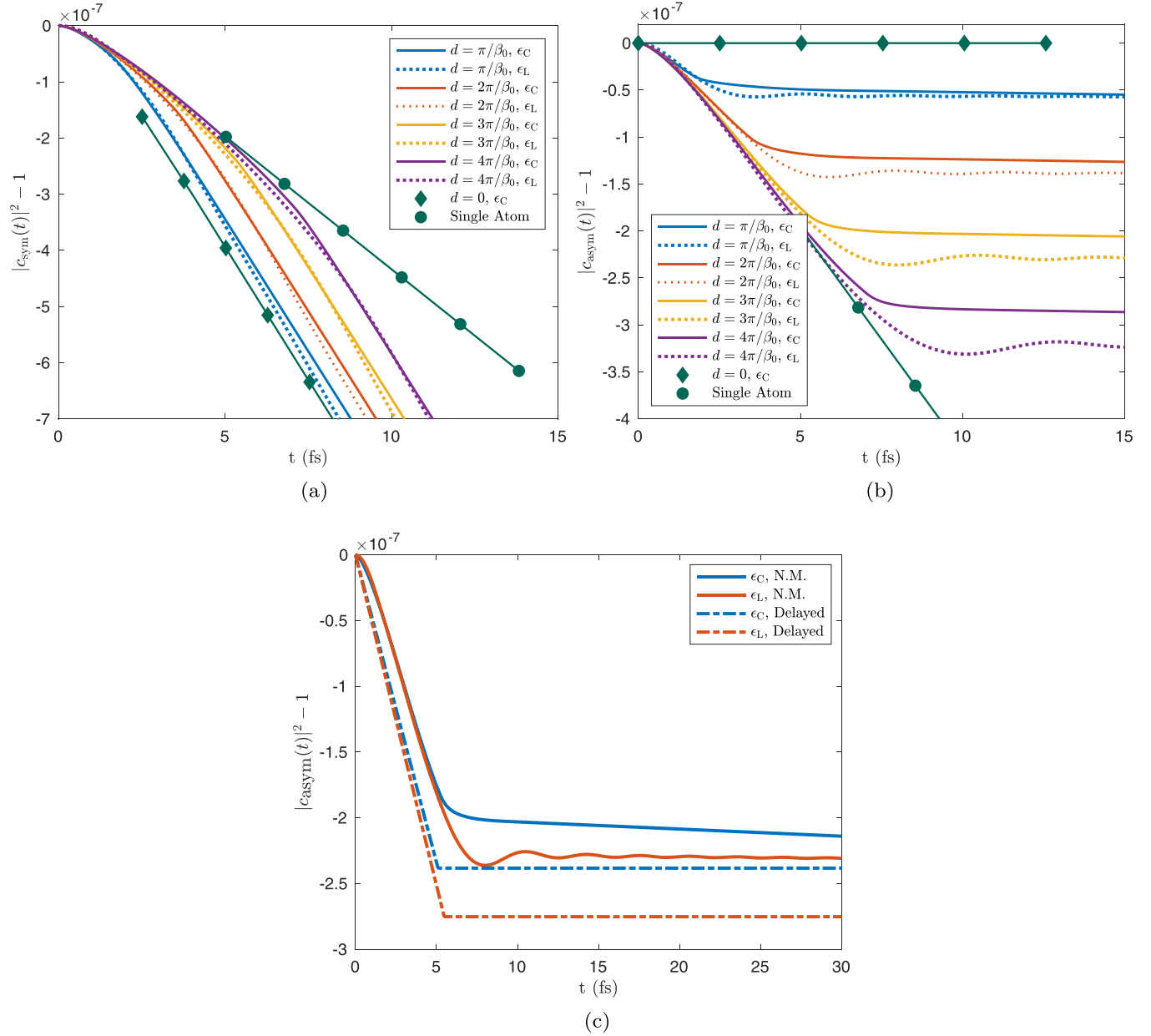


FIG. 5. Collective excitation probabilities for initial symmetric (a) and antisymmetric (b) states for atoms 100 nm away from a 200 nm radius ONF for several equilibrium separations $d_{\text{eq}} = n\pi/\beta_0$. In both panels the solid curves refer to the emission probabilities using the constant dielectric function, while the dashed ones depict those obtained with the DL dielectric function. Note that the transition from independent to collective decay is smooth, taking a longer time for the DL dielectric function. In (c) we compare the collective excitation probabilities calculated with different correlation functions for an antisymmetric state for atoms separated at $3\pi/\beta_0$ using both dielectric functions. The solid curves result from ONF's correlation functions, while the dashed ones were obtained using displaced Dirac delta correlations. Using Dirac delta correlations we obtain an instantaneous establishment of a not decaying collective behavior. For the other two correlation functions the collective behavior continues to decay, although slowly.

C. Onset of the collective decay

Figure 5 shows that it is unclear when the collective behavior is fully established. In Ref. [18] the transition from independent emitters to the collective regimes occurs instantaneously at the time $t = d/v_g(\omega_0)$, which is the time displacement between the Dirac deltas in the correlation functions, commonly introduced *ad hoc*. To estimate a time where the collective behavior starts, we extrapolate to earlier times the exponential decay observed at times beyond 300 fs and

define the communication time t_{com} to be that at which the single atom and the approximated long-time collective emission probabilities intersect. Figure 7(a) shows an example of this procedure, and Fig. 7(b) portrays the communication rate $v_{\text{com}} = d/t_{\text{com}}$ as a function of the separation between atoms, the ONF radius, and both dielectric functions. We find that v_{com} is independent of the initial state of the atoms and that deviations from the group velocity are significant only for separations less than the atomic resonant wavelength

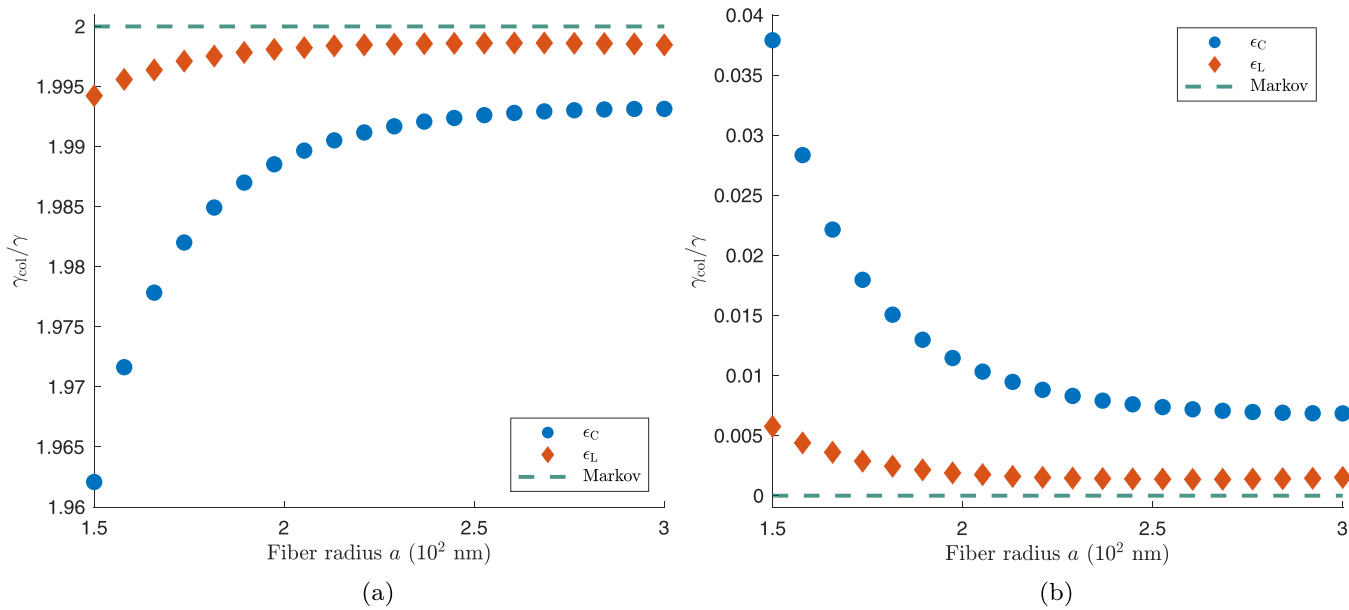


FIG. 6. Collective decay rates of superradiant (a) and subradiant (b) atoms (normalized with respect to the decay rate of an independent atom in the vicinity of the ONF, γ) separated at the resonant atomic wavelength $d = 2\pi/\beta_0 = 780$ nm and at 100 nm away from the ONF's surface as a function of the fiber's radius. In both panels the circular dots depict the collective rates using the constant function, while the diamonds portray the results obtained with the DL dielectric function.

$\lambda_0 = 2\pi/\beta_0$, the exception being the rates calculated with the DL function for a 150 nm ONF, which are attributable to the significant oscillations in its correlation functions. This offers a satisfactory justification for approximating the correlation function with two Dirac delta peaks separated by the time the field propagates between the atoms at group velocity even if it

is the phase velocity that appears in the Hamiltonian through its relation to the propagation constant $\beta(\omega)$.

To estimate the time to establish the collective behavior t_{Est} , we account for the fact that the solutions vary insignificantly in magnitude during the transition from the independent to the collective behavior, and, thus, we extract

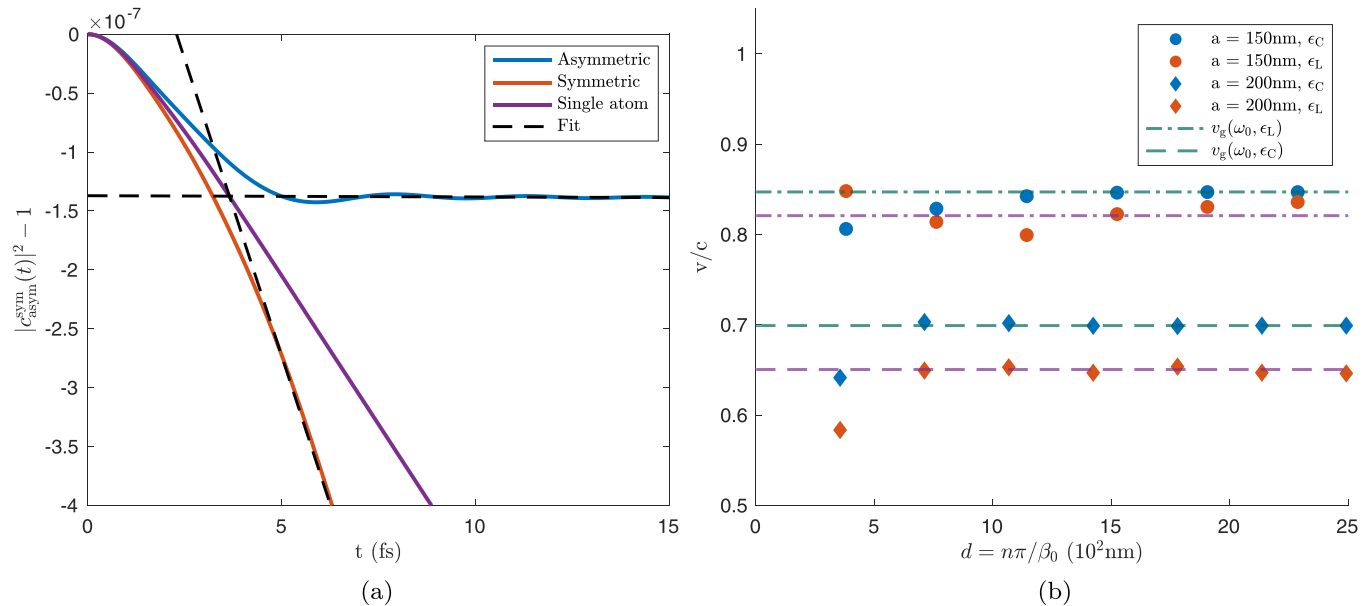


FIG. 7. (a) Intersection of the linearized collective emission probabilities for initially symmetric (lower curve) and antisymmetric (upper curve) atomic states with the single-atom emission probability for atoms separated at their resonant wavelength $d = 2\pi/\beta_0$ at 100 nm away from the surface of a 200 nm radius ONF modeled with the DL dielectric function ϵ_L . (b) Atom-atom communication speed for atoms separated at integer multiples of π/β_0 at 100 nm away from the ONF's surface. The circular dots and rhombuses portray the results for a 150 nm and a 200 nm fiber's radius, respectively. The dashed horizontal lines are the group velocities for the atom's resonant frequency and a given dielectric function. The speeds are normalized with respect to the speed of light in vacuum.

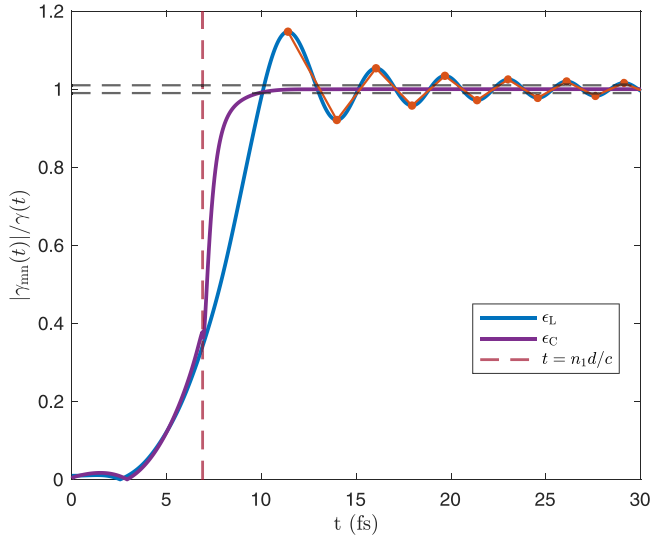


FIG. 8. Absolute value of the spontaneous decay rate of an atom due to the influence of the second $\gamma_{mn}(t) = \int_0^t dt' \text{Re}[F_{mn}(t-t')]$ [normalized with respect to the decay rate of an independent atom in the vicinity of the ONF, $\gamma(t)$] for atoms separated at twice the atomic resonant wavelength $d = 4\pi/\beta_0$ at 100 nm away from the surface of a 200 nm ONF for both dielectric functions. The dots represent the local maxima and minima of the curve obtained with the DL function, and the time of establishment of the collective regime t_{Est} in this case is defined as that at which the middle point of the line connecting two successive maximum and minimum lies within 0.01 from $|\gamma_{mn}(t)|/\gamma(t) = 1$. For the constant dielectric function, we consider the establishment time to be when the quotient reaches 0.99. For separations much smaller than the coherence length of a superradiant photon $l_{\text{coh}} = v_g(\omega_0)/\gamma_{\text{sup}}$, there is an eight orders of magnitude difference between the timescale of transitioning from independent to collective emission (10^{-15} s) and the single-atom emission into the guided mode of the nanofiber (10^{-7} s). This difference indicates that the transition between the independent and collective regimes is irrelevant to the overall dynamics of the atoms.

the probability amplitudes in Eq. (6) out of the time integral and study the behavior of the correlation functions integrals. Considering this and the fact that the imaginary parts of the correlation approach their asymptotic behavior in the same timescales as their real counterparts, the evolution equations become

$$\dot{c}_m(t) = -[\gamma_{mm}(t)c_m(t) + \gamma_{mn}(t)c_n(t)], \quad (9)$$

$$\gamma_{mn}(t) = \int_0^t dt' \text{Re}[F_{mn}(t-t')]. \quad (10)$$

Here, in correspondence to the results obtained with the Markovian approximation [26], the collective decay rates of (anti-) symmetric states are given by

$$\gamma_{\mp}(t) = \gamma(t) \mp |\gamma_{mn}(t)|, \quad (11)$$

which in case of the Markovian approximation and separations which are integer multiples of π/β_0 , $|\gamma_{mn}| = \gamma$, and thus, these states correspond to a (sub-) superradiant emission. Figure 8 depicts the time-dependent quotient of the decay rates $|\gamma_{mn}(t)|/\gamma(t)$ for atoms separated at twice their

resonant wavelength and 100 nm away from the surface of a 200 nm radius ONF for both dielectric functions. When using the constant dielectric function, the quotient becomes 1 for times greater than $t = dn_1/c$, and the time of establishment of the collective behavior is regarded as the time the quotient reaches 0.99. Meanwhile, for the DL function, the quotients calculated for different separations grow to a maximum and converge asymptotically towards 1 as $t \rightarrow \infty$ while oscillating. In this case, we define the time to establish the collective behavior as the time at which the midpoint of the line joining two successive maximum and minimum of the curve lies within a range less than 0.01 from $|\gamma_{mn}(t)|/\gamma(t) = 1$, as shown in Fig. 8. Figure 9 shows the time to establish the collective decay for both dielectric functions normalized with respect to the time a photon propagates between the atoms moving at the group velocity, which we denote as $t_{v_g} = d/v_g(\omega_0)$. The results are shown as a function of the separation between the atoms and the ONF's radius. Again, we find the time to establish collective behavior is independent of the initial atomic state and that it decreases to values less than $2t_{v_g}$ when employing the DL function, and almost to t_{v_g} when considering the constant dielectric function. Thus, when the atoms are separated several times their resonant wavelength, the distinction between the independent and collective regimes is established in a time smaller than $2t_{v_g}$.

IV. CONCLUSIONS

In this work we analyzed the correlation functions of the electromagnetic environment provided by the fundamental guided mode of an optical nanofiber. We studied their effects on the collective dynamics of two separated two-level atoms. The width and central position of the correlation functions depend strongly on the dispersion relation of the waveguide. The correlation functions resemble nascent delta distributions when considering a constant dielectric function. Still, the time difference between their peaks does not coincide with the time that would take for the field to propagate between the two atoms propagating at group or phase velocity. Nevertheless, when studying the dynamics of the atoms, we found that approximating the correlation function with two Dirac delta functions separated by the time the field propagates between the atoms at group velocity is a good approximation, provided the atoms are placed far enough. When the atoms are just a few wavelengths apart, the intuition from a well-defined traveling wave package breaks down, and it becomes hard to define a unique characteristic timescale to establish collective behavior. We obtained the collective excitation probabilities of super- and subradiant atoms by solving their Schrödinger equation in the non-Markovian regime and found that the collective decay rates can differ by less than 5% and 1% compared to the Markovian approximation when considering a constant and Drude-Lorentz dielectric functions, respectively. We conclude that the Markov approximation is good enough for state-of-the-art experiments involving atoms around optical nanofibers. However, its validity must be examined in other waveguide QED platforms, considering their particular dielectric function, dispersion relation, and the level of precision the experiments might require.

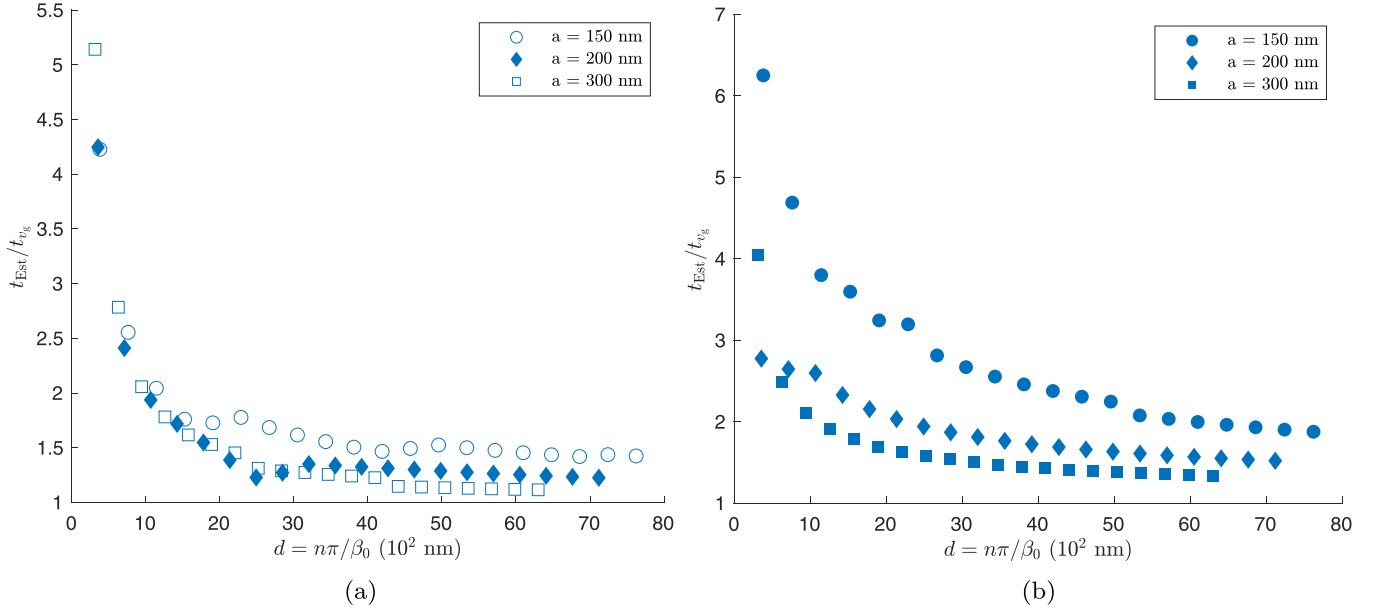


FIG. 9. Times of establishment of the collective decay t_{Est} for the constant ϵ_C (a) and the DL ϵ_L (b) dielectric functions. The atoms are separated at integer multiples of π/β_0 and at 100 nm away from the fiber's surface. The results are normalized with respect to the travel time of a photon moving between the atoms at the group velocity $t_{v_g} = d/v_g(\omega_0)$.

ACKNOWLEDGMENTS

We thank K. Sinha for insightful discussions. P.S. is a CIFAR Azrieli Global Scholar in the Quantum Information Science Program. This work was supported in part by CONICYT-PAI Grant No. 77190033, FONDECYT Grant No. 11200192 from Chile, and DGAPA-PAPIIT Grant No. IG101421 from UNAM, Mexico.

APPENDIX: SOLUTION OF THE EQUATIONS

In order to solve the dynamical equations of the atomic probability amplitudes

$$\dot{c}_m(t) = - \sum_{n=1}^2 \int_0^t dt' F_{mn}(t-t') c_n(t'), \quad (\text{A1})$$

we transform them into a linear system of equations by means of the trapezoidal rule [33]. First, we integrate both sides of Eq. (A1) between two successive points of the Fourier transform time grid t_j , t_{j+1} , yielding

$$c_m^{j+1} = c_m^j - \sum_{n=1}^2 \int_{t_j}^{t_{j+1}} dt \int_0^t dt' F_{mn}(t-t') c_n(t'). \quad (\text{A2})$$

Then, applying the trapezoidal rule

$$\int_a^b dt f(t) = \frac{h}{2} \left[2 \sum_{k=2}^{N-1} f(t_k) + f(t_N) + f(t_1) \right] + O(h^3) \quad (\text{A3})$$

twice on the right-hand side of Eq. (A2) allows us to recursively solve for the probability amplitudes in terms of the following system:

$$M\bar{x} = \bar{y}, \quad (\text{A4})$$

$$\bar{x}^T = [a_1^{j+1}, a_2^{j+1}, b_1^{j+1}, b_2^{j+1}], \quad (\text{A5})$$

$$M = \mathbf{Id}$$

$$+ \left(\frac{h}{2}\right)^2 \begin{bmatrix} A(1,1) & -B(1,1) & C(1,1) & -D(1,1) \\ B(1,1) & A(1,1) & C(1,1) & D(1,1) \\ C(1,1) & -D(1,1) & A(1,1) & -B(1,1) \\ D(1,1) & C(1,1) & B(1,1) & A(1,1) \end{bmatrix}, \quad (\text{A6})$$

where \mathbf{Id} is the 4×4 identity matrix, $h = t_{j+1} - t_j$, $\forall j$, and

$$A(j,k) = \text{Re}[F_{mn}(t_j - t_k)], \quad B(j,k) = \text{Im}[F_{mn}(t_j - t_k)], \quad (\text{A7})$$

$$C(j,k) = \text{Re}[F_{mn}(t_j - t_k)], \quad D(j,k) = \text{Im}[F_{mn}(t_j - t_k)], \quad (\text{A8})$$

$$a_1^j = \text{Re}[c_m(t_j)], \quad a_2^j = \text{Im}[c_m(t_j)], \quad (\text{A9})$$

$$b_1^j = \text{Re}[c_n(t_j)], \quad b_2^j = \text{Im}[c_n(t_j)], \quad (\text{A10})$$

refer to the real Re and imaginary Im parts of both the correlation functions and the atomic probability amplitudes; the vector \bar{y} , which takes into account the present and past states of the atomic amplitudes, is defined as

$$\bar{y} = \begin{pmatrix} [1 - Y^A]a_1^j - [X_{a_1}^A - X_{a_2}^B + X_{b_1}^C - X_{b_2}^D] - [Y^B a_2^j - Y^C b_1^j + Y^D b_2^j] \\ [1 - Y^A]a_2^j - [X_{a_2}^A - X_{a_1}^B + X_{b_2}^C - X_{b_1}^D] - [Y^B a_1^j - Y^C b_2^j + Y^D b_1^j] \\ [1 - Y^A]b_1^j - [X_{b_1}^A - X_{b_2}^B + X_{a_1}^C - X_{a_2}^D] - [Y^B b_2^j - Y^C a_1^j + Y^D a_2^j] \\ [1 - Y^A]b_2^j - [X_{b_2}^A - X_{b_1}^B + X_{a_2}^C - X_{a_1}^D] - [Y^B b_1^j - Y^C a_2^j + Y^D a_1^j] \end{pmatrix}, \quad (\text{A11})$$

$$Y^F = \left(\frac{\hbar}{2}\right)^2 [2F(2, 1) + F(1, 1)], \quad (\text{A12})$$

$$X_d^F = \left(\frac{\hbar}{2}\right)^2 \left\{ 2 \sum_{l=2}^{j-1} [F(j+1, l) + F(j, l)] d^l + [F(j+1, 1) + F(j, 1)] d^1 \right\}. \quad (\text{A13})$$

-
- [1] H. J. Carmichael, *Statistical Methods in Quantum Optics I: Master Equations and Fokker-Planck Equations* (Springer, 2002).
- [2] H. J. Carmichael, *An Open Systems Approach to Quantum Optics* (Springer-Verlag, Berlin, Heidelberg, 1993).
- [3] A. Rivas and S. F. Huelga, *Open Quantum Systems*, Springer Briefs in Physics, Vol. 10 (Springer, 2012).
- [4] I. de Vega and D. Alonso, *Rev. Mod. Phys.* **89**, 015001 (2017).
- [5] R. Alicki and K. Lendi, *Quantum Dynamical Semigroups and Applications*, Vol. 717 (Springer, Berlin, Heidelberg, 2007).
- [6] H.-P. Breuer and F. Petruccione, *Theory of Open Quantum Systems* (Oxford University Press, New York, 2002).
- [7] G. S. Agarwal, *Quantum Optics*, edited by G. Höhler, Springer Tracts in Modern Physics, Vol. 70 (Springer, Berlin, Heidelberg, 1974), pp. 1–128.
- [8] P. G. Brooke, K.-P. Marzlin, J. D. Cresser, and B. C. Sanders, *Phys. Rev. A* **77**, 033844 (2008).
- [9] A. S. Sheremet, M. I. Petrov, I. V. Iorsh, A. V. Poshakinskiy, and A. N. Poddubny, *Rev. Mod. Phys.* **95**, 015002 (2023).
- [10] A. Johnson, M. Blaha, A. E. Ulanov, A. Rauschenbeutel, P. Schneeweiss, and J. Volz, *Phys. Rev. Lett.* **123**, 243602 (2019).
- [11] H. S. Han, A. Lee, K. Sinha, F. K. Fatemi, and S. L. Rolston, *Phys. Rev. Lett.* **127**, 073604 (2021).
- [12] M. Mirhosseini, E. Kim, X. Zhang, A. Sipahigil, P. B. Dieterle, A. J. Keller, A. Asenjo-Garcia, D. E. Chang, and O. Painter, *Nature (London)* **569**, 692 (2019).
- [13] P. Y. Wen, K.-T. Lin, A. F. Kockum, B. Suri, H. Ian, J. C. Chen, S. Y. Mao, C. C. Chiu, P. Delsing, F. Nori *et al.*, *Phys. Rev. Lett.* **123**, 233602 (2019).
- [14] J.-H. Kim, S. Aghaeimeibodi, C. J. K. Richardson, R. P. Leavitt, and E. Waks, *Nano Lett.* **18**, 4734 (2018).
- [15] P. Solano, P. Barberis-Blostein, F. K. Fatemi, L. A. Orozco, and S. L. Rolston, *Nat. Commun.* **8**, 1857 (2017).
- [16] A. Goban, C.-L. Hung, J. D. Hood, S.-P. Yu, J. A. Muniz, O. Painter, and H. J. Kimble, *Phys. Rev. Lett.* **115**, 063601 (2015).
- [17] A. Asenjo-Garcia, M. Moreno-Cardoner, A. Albrecht, H. J. Kimble, and D. E. Chang, *Phys. Rev. X* **7**, 031024 (2017).
- [18] K. Sinha, P. Meystre, E. A. Goldschmidt, F. K. Fatemi, S. L. Rolston, and P. Solano, *Phys. Rev. Lett.* **124**, 043603 (2020).
- [19] K. Sinha, A. González-Tudela, Y. Lu, and P. Solano, *Phys. Rev. A* **102**, 043718 (2020).
- [20] P. Solano, P. Barberis-Blostein, and K. Sinha, *Phys. Rev. A* **107**, 023723 (2023).
- [21] J.-T. Shen and S. Fan, *Phys. Rev. Lett.* **95**, 213001 (2005).
- [22] H. Zheng and H. U. Baranger, *Phys. Rev. Lett.* **110**, 113601 (2013).
- [23] A. Carmele, N. Nemet, V. Canela, and S. Parkins, *Phys. Rev. Res.* **2**, 013238 (2020).
- [24] A. Olivera, K. Sinha, and P. Solano, *Phys. Rev. A* **106**, 013703 (2022).
- [25] P. Solano, J. A. Grover, J. E. Hoffman, S. Ravets, F. K. Fatemi, L. A. Orozco, and S. L. Rolston, *Adv. At. Mol. Opt. Phys.* **66**, 439 (2017).
- [26] F. Le Kien, S. DuttaGupta, K. P. Nayak, and K. Hakuta, *Phys. Rev. A* **72**, 063815 (2005).
- [27] Á. Rivas, A. D. K. Plato, S. F. Huelga, and M. B. Plenio, *New J. Phys.* **12**, 113032 (2010).
- [28] J. D. Jackson, *Classical Electrodynamics*, 3rd ed. (Wiley & Sons, New York, 1999).
- [29] D. Marcuse, *Light Transmission Optics*, Van Nostrand Reinhold Electrical/Computer Science and Engineering Series, 2nd ed. (Krieger Publishing Company, New York, 1989).
- [30] H. Carmichael, *Statistical Methods in Quantum Optics I: Master Equations and Fokker-Planck Equations*, Physics and Astronomy Online Library (Springer, Berlin, Heidelberg, 1999).
- [31] K. Lindenberg and B. J. West, *Phys. Rev. A* **30**, 568 (1984).
- [32] P. Solano, J. A. Grover, Y. Xu, P. Barberis-Blostein, J. N. Munday, L. A. Orozco, W. D. Phillips, and S. L. Rolston, *Phys. Rev. A* **99**, 013822 (2019).
- [33] W. H. Press, B. P. Flannery, S. A. Teukolsky, and W. T. Vetterling, *Numerical Recipes in FORTRAN 77: The Art of Scientific Computing* (Cambridge University Press, New York, 1992).